BULETINUL INSTITUTULUI POLITEHNIC DIN IAŞI
Publicat de
Universitatea Tehnică „Gheorghe Asachi” din Iaşi
Volumul 68 (72), Numărul 4, 2022
Secţia
CONSTRUCŢII DE MAŞINI
DOI:10.2478/bipcm-2022-0038

A STUDY OF 2D PROFILE FOR A CYCLOIDAL RING USED IN A CYCLOIDAL REDUCER

BY

MIHĂIŢĂ HORODINCĂ*, EDUARD NECULAI BUMBU, DRAGOŞ FLORIN CHITARIU, ADRIANA MUNTEANU, FLORIN CHIFAN and GEORGE IULIAN FRIGURA

“Gheorghe Asachi” Technical University of Iaşi,
Faculty of Machine Manufacturing and Industrial Management

Received: December 23, 2022
Accepted for publication: December 29, 2022

Abstract. This paper intends to introduce a new approach in cycloidal reducers design. The usual design uses rotary pins as teeth on the ring gear (or stator as well) and an appropriate conjugate profile on the cycloidal disc (or rotor as well). This study proposes a new approach: to use rotary cylindrical pins as teeth on the rotor and an appropriate conjugate profile on the ring gear (or cycloidal ring) according with the rules of gearing. The main achievements of this paper focus on the synthesis of 2D internal profile of the cycloidal ring in transverse section. Some theoretical achievements and computer aided simulation results are briefly presented in this paper. This 2D profile is useful mainly for cycloidal reducer computer aided simulation and optimization but also for manufacturing purposes (by contour milling on CNC machines).

Keywords: Cycloidal reducer, rotary pins on rotor, cycloidal ring, 2D profile, computer aided synthesis.

*Corresponding author; *e-mail*: horodinca@tuiasi.ro.

1. Introduction

In the last decade the cycloidal reducers (CR) became frequently an interesting option in industrial applications due to their notable performances: compact and robust design, low gear ratio, high output torque, high power efficiency, especially when it uses rotary cylindrical pins inside as gear teeth placed on the ring gear. The actually design of CR uses a fixed ring gear (as stator) having (rarely) fixed or (frequently) cylindrical rotary pins (sometimes replaced by bearings) playing the role of Z_S equidistant gear teeth. A rotary rotor (acting as a planet gear) having an appropriate external shape (with Z_R lobes as gear teeth) is placed on a carrier (with certain eccentricity) being permanently in internal gearing with the stator. The carrier rotation (around a fixed end) works as input rotary motion (with n_{in} as rotary speed), the rotor rotation around its (movable) axis (being placed on the rotary end of the carrier) is the output rotary motion (as reverse gear), with n_{out} as rotary speed. If $Z_R = Z_S - 1$ (a specific relationship inside the CR) then the lowest possible gear ratio is mathematically simply describable as:

$$\frac{n_{out}}{n_{in}} = -\frac{1}{Z_R} \tag{1}$$

There are two major challenges in classically CR design and manufacturing. First challenge -simpler- is to transfer the output motion (around a rotary axis) to a shaft with fixed axis. Second challenge -more complicated- is to obtain (as design and manufacture) an appropriate external shape of the rotor (cycloidal disc). The correct mathematical description of this shape is important for manufacturing, based usually on 2D contour milling on CNC machines. It is also important in order to facilitate the optimization of some parameters of this shape (*e.g.* 2D profile shifting) for increasing the power efficiency (Wang *et al*., 2019; Allota *et al.*, 2021; Mackic, 2013) or to control the values and the distribution of contact forces (Huang and Tsai, 2017).

An interesting study about the parametric definition of the 2D profiles of the cycloidal discs was proposed by (Shin and Kwon, 2006). In 2013 (Petrovic *et al.*) introduces a mathematical definition of these profiles (called also epitrochoid curves) and some computer programs for simulation. Some achievements related by cycloidal gears profiles useful in pumps were presented in (Litvin and Feng, 1996). In a previous work (Horodincă *et al*., 2022) was proposed a method to define this 2D profile as the internal envelope of the family of curves (epicycloids) generated by the ring gear which completely rotates around a fixed rotor. Some similarities with this approach were also previously proposed in (Horodincă, 2020) for synthesis of internal cylindrical gears with sinusoidal profile.

A consequence which completes these previous works is this new study simply formulated as follows: a new conception of a CR is possible if the rotary

cylindrical pins are moved from the stator (ring gear) on the rotor. Of course now the internal shape of the ring gear should be appropriate in gearing with the pins (shape and movement) from the rotor. It is easy to anticipate that the stator 2D profile is associated with a hypocycloid (this will be proved later on). This is the reason why the stator can be suggestively renamed as cycloidal ring.

It is possible that this new approach on CR design has some advantages as against the current design; this will be a future challenge in our work. However a simple observation is available: the new design needs only Z_R rotary pins placed on rotor, by comparison with $Z_S=Z_R+1$ rotary pins necessary to be placed on stator in the current design.

In a summary approach it is possible to define the internal cycloidal ring 2D profile, as the external envelope of the family of curves (hypocycloids) generated by the rotor during at least Z_R completely rotations of the carrier around its fixed axis. Similarly with the theoretical achievements from the previous work (Horodincă *et al.*, 2022) a simpler approach in this paper defines this cycloidal ring 2D profile as the envelope of all positions of the rotor pins during the same Z_R completely rotations. Some theoretical considerations related by mathematical description of rotor motion (which helps to define these rotor pins positions and to find out the description of the cycloidal ring 2D profile) and some computer aided simulation will be detailed in this work.

Section 2 of this paper presents a theoretical approach on the rotor motion related to the stator. Some results on simulations of the positions for 2D rotary pins profiles are described in Section 3. Section 4 presents the detection method of the coordinates of external envelope of these positions with some results by simulation. Section 5 presents a view with a 3D CAD model of a cycloidal ring (having the transverse section defined in an example from Section 4) and a formal gearing with the rotor. Section 6 presents the conclusions and the future work.

2. A theoretical approach on the rotor motion relative to the stator

Figure 1 presents conceptually the working principle of a CR. The stator (the ring gear) is firmly attached to a fixed circle (S) having the radius r_S (as basic circle). The rotor is firmly attached to a circle (R) having the radius r_R (as rolling circle). These circles are permanently tangents at the interior in the point P_t (no relative speed there, the rolling circle moves without slipping inside the basic circle). The circle (R) has the center placed in the point O_2, the rotary end of a carrier Cr. This point O_2 has a rotary motion, its trajectory being a circle (with the radius $r_S - r_R$) with the center in the fixed end O_1 of the carrier. The eccentricity of the carrier Cr is mandatory expressed as $d_{O_1-O_2} = r_S - r_R$. The carrier has a rotary motion around the point O_1 (here supposed to be in counterclockwise, CCW) with the input rotary speed n_{in}. As consequence, the circle (R) rotates around the point O_2 (in clockwise, CW) with the output speed

n_{out} (the output motion is mandatory in opposite direction as against to the input motion). The gear ratio n_{out}/n_{in} is describable with a well-known relationship (Eq. (2) written below) between radii (Petrovic *et al.*, 2013). Because the radii r_S and r_R are proportional with the numbers of teeth Z_R and Z_S (and the gear module m as well) and because $Z_S - Z_R = 1$, finally the gear ratio from Eq. (2) is expressed identically with Eq. (1).

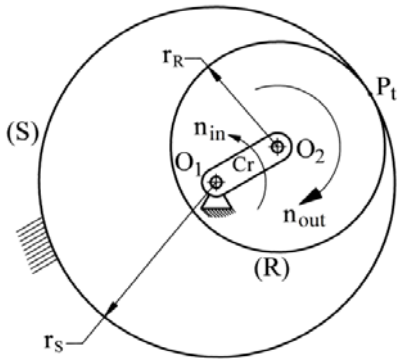

Fig. 1 – An approach on the working principle of a cycloidal reducer.

$$\frac{n_{out}}{n_{in}} = -\frac{r_S - r_R}{r_R} = -\frac{mZ_S - mZ_R}{mZ_R} = -\frac{Z_S - Z_R}{Z_R} = -\frac{1}{Z_R} \tag{2}$$

From Eq. (2) results this mandatory relationship between r_R and r_S radii:

$$r_S = r_R\left(1 + \frac{1}{Z_R}\right) \tag{3}$$

If the carrier Cr rotates with an angle α around the point O_1 than the circle (R) -or the CR rotor as well- rotates with an angle β around the point O_2. Of course, any point placed on the rotor (particularly a point placed on a rotary pin, if the pin rotation around its axis is ignored) rotates with the same angle β. It is obvious that the equality $\beta/\alpha = n_{out}/n_{in}$ allows to express the angle β as:

$$\beta = -\frac{\alpha \cdot (r_S - r_R)}{r_R} = -\frac{\alpha}{Z_R} \tag{4}$$

As consequence of Eq. (4), is mandatory to accomplish the relationship $Z_R = r_R/(r_S - r_R)$ in a CR design.

3. A theoretical approach on the simulation of the positions for 2D profiles of the rotary pins placed on the rotor

Suppose that x_{Rm} and y_{Rm} are the 2D coordinates of a generic point placed on the CR rotor in a mobile coordinate Cartesian system (as MCCS)

attached to the rotor, having the origin in O_2. Particularly this point can be placed on a rotary pin (its rotary motion being ignored). Considering the operation of the reducer under the above conditions, the abscissa x_{Rf} of this generic point in a fixed coordinate Cartesian system (as FCCS) having the origin in O_1 can be described with the parametric equation:

$$x_{Rf}(\alpha) = (r_S - r_R) \cdot \cos(\alpha) + x_{Rm} \cdot \cos\left(\frac{\alpha}{Z_R}\right) + y_{Rm} \cdot \sin\left(\frac{\alpha}{Z_R}\right) \qquad (5)$$

The first term in the right-hand side of Eq. (5) is the abscissa of the point O_2 in FCCS (a consequence of carrier rotation with angle α). The second and the third terms describe the projection on FCCS x-axis of the generic point considering that MCCS rotates with an angle $\beta=-\alpha/Z_R$.

Similarly, the ordinate y_{Rf} of this generic point in the same FCCS can be described with the parametric equation:

$$y_{Rf}(\alpha) = (r_S - r_R) \cdot \sin(\alpha) + y_{Rm} \cdot \cos\left(\frac{\alpha}{Z_R}\right) - x_{Rm} \cdot \sin\left(\frac{\alpha}{Z_R}\right) \qquad (6)$$

The first term in the right-hand side of Eq. (6) is the ordinate of the point O_2 in FCCS (also a consequence of carrier rotation with angle α). The second and the third terms describe the projection on FCCS y-axis of the generic point considering also that MCCS rotates with an angle $\beta=-\alpha/Z_R$.

Suppose that the rotary pins centers (having the radius r_p) from the rotor are placed on a circle (P) with the radius r_{pp} centred in O_2. Suppose that in an imaginary mode there are $2 \cdot Z_R$ side by side tangents pins on rotor, each one having the center placed on the circle (P). These $2 \cdot Z_R$ pins are distributed so that they covers completely the entire circumference of the circle (P). Then here is this evident relationship between the radii r_p and r_{pp}:

$$\frac{r_p}{r_{pp}} = \sin\left(\frac{2\pi}{4Z_R}\right) \qquad (7)$$

In this work an option in CR design is to use from these $2 \cdot Z_R$ pins only Z_R angular equidistant pins.

If the radius r_p is imposed (*e.g.* as being the radius of a bearing playing the role of a rotary pin) then the radius r_{pp} of circle (P) is provided by Eq. (7) as:

$$r_{pp} = \frac{r_p}{\sin\left(\frac{\pi}{2Z_R}\right)} \qquad (8)$$

With circles (P) and (R) firmly fixed together (having the same center O_2) a generic point x_{Rm} and y_{Rm} in MCCS placed in the center O_3 of a 2D profile of a rotary pin (as circle) has the coordinates:

$$x_{Rm} = x_{O_3 m} = r_{pp} \cdot \cos(\gamma_f) \qquad y_{Rm} = y_{O_3 m} = r_{pp} \cdot \sin(\gamma_f) \qquad (9)$$

Here γ_f is a fixed angle value. The other pins are placed equidistantly at angles $2\cdot\gamma_f$, $3\cdot\gamma_f$ …$Z_R\cdot\gamma_f$ on the circle (P). With the definitions from Eq. (9) used in Eq. (5) and (6) the parametric equations of the trajectory of this point O_3 in FCCS become:

$$x_{O_3f}(\alpha) = (r_S - r_R)\cos(\alpha) + r_{pp}\cos(\gamma_f)\cos\left(\frac{\alpha}{Z_R}\right) + r_{pp}\sin(\gamma_f)\sin\left(\frac{\alpha}{Z_R}\right) \tag{10}$$

$$y_{O_3f}(\alpha) = (r_S - r_R)\sin(\alpha) + r_{pp}\sin(\gamma_f)\cos\left(\frac{\alpha}{Z_R}\right) - r_{pp}\cos(\gamma_f)\sin\left(\frac{\alpha}{Z_R}\right) \tag{11}$$

If there is a perfect overlap between the circles (P) and (R), with $r_R=r_{pp}$ the trajectory of point O_3 is mandatory a closed hypocycloid (as (H_{Cp}), generated by a center of a rotary pin), because O_3 is a point on an inner circle that rolls inside the circle (S). This hypocycloid (having $Z_S = Z_R + 1 = r_R/(r_S - r_R) + 1$ cusps or sharp corners) is inscribed in the circle (S). This conclusion is proved by simulation in Fig. 2, where the hypocycloid is generated for $Z_R=9$ rotary pins (having 10 cusps) on the rotor having $r_p=5$ *mm*. Eq. (8) produces $r_{pp}=r_R = 28.7939$ *mm*, Eq. (3) produces $r_S=31.9932$ *mm*. The angle α evolves in CCW (CW) between *0* and $2\pi Z_R$ (for Z_R full rotations of the carrier Cr) while the angle β evolves in CW (CCW) between *0* and 2π (for a full rotation of the rotor around its center O_2), the angle γ_f was (arbitrary) chosen as being $\gamma_f=\pi$.

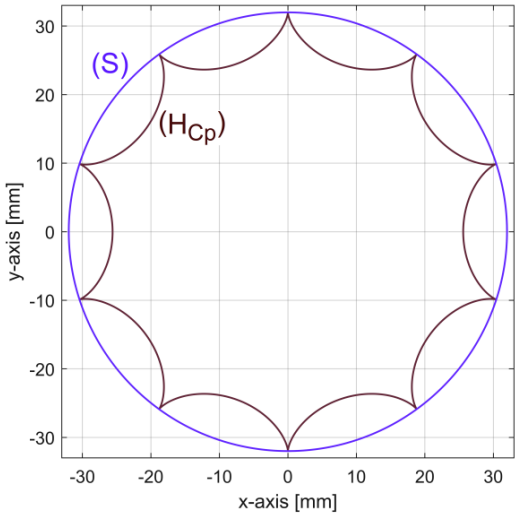

Fig. 2 – An example of closed hypocycloid (H_{Cp}) generated by a center O_3 of a rotary pin placed on the rotor during Z_R full rotations of the carrier inside a CR ($Z_R=9$, $r_p=5$ *mm*, $r_{pp}=r_R=28.7939$ *mm*, $\gamma_f=\pi$ and $r_S=31.9932$ *mm*).

Let be the 2D coordinates x_{Rpm} and y_{Rpm} in MCCS of a generic point placed on the 2D profile of a rotary pin (as circle with radius r_p with the center in O_3 previously used in Eq. (9)) written as:

$$x_{Rpm}(\delta) = r_{pp}\cos(\gamma_f) + r_p\cos(\delta) \quad \text{and} \quad y_{Rpm} = r_{pp}\sin(\gamma_f) + r_p\sin(\delta) \tag{12}$$

If the angle δ evolves between 0 and 2π then a 2D profile of a rotary pin profile is obtained.

A position of the 2D rotary pin profile on the (H_{Cp}) hypocycloid (for a certain value of the angle $\alpha=\alpha_f$) is obtained if the coordinates MCCS x_{Rpm} and y_{Rpm} from Eq. (12) are transferred in FCCS, in other words if these coordinates (with δ evolving between 0 and 2π) are transferred in FCCS (as x_{Rpf} and y_{Rpf}) through the Eq. (5) and (6) as follows:

$$x_{Rpf}(\alpha_f) = (r_S - r_R)\cos(\alpha_f) + x_{Rpm}(\delta)\cos\left(\frac{\alpha_f}{Z_R}\right) + y_{Rpm}(\delta)\sin\left(\frac{\alpha_f}{Z_R}\right) \tag{13}$$

$$y_{Rpf}(\alpha_f) = (r_S - r_R)\sin(\alpha_f) + y_{Rpm}(\delta)\cos\left(\frac{\alpha_f}{Z_R}\right) - x_{Rpm}(\delta)\sin\left(\frac{\alpha_f}{Z_R}\right) \tag{14}$$

If α_f has an incremental variation between 0 and $2\pi Z_R$, for each value α_f then a position of the 2D rotary pin profile on the (H_{Cp}) hypocycloid is obtained (if δ evolves between 0 and 2π for each α_f value). This is proved by simulation in Fig. 3 (a completion of Fig. 2). An incremental variation $\Delta\alpha_f=2\pi/50$ was used in Eq. (13) and (14), so a number of $50Z_R=450$ equidistant 2D rotary pin profiles (depicted in cyan color) were obtained and depicted in Fig. 3.

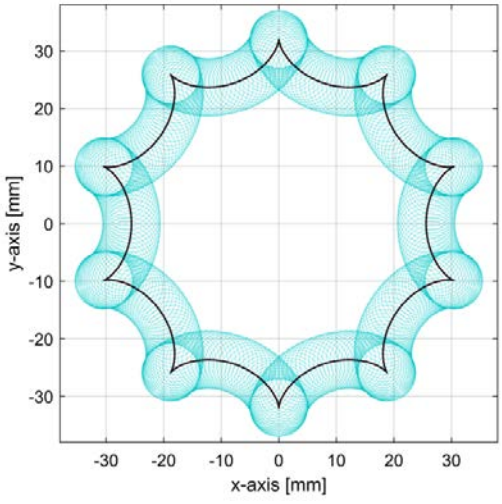

Fig. 3 – A completion of Fig. 2 with 450 positions of the 2D rotary pin profiles placed on (H_{Cp}) hypocycloid.

If $\Delta\alpha_f$ in Eq. (13) and (14) tends to zero ($\Delta\alpha_f \rightarrow 0$) then the cyan colored surface from Fig. 3 is completely covered, all possible positions of those Z_R 2D rotary pin profiles placed on the rotor are depicted for a full rotation of the carrier Cr. If after that Eq. (13) and (14) are applied again but for $\Delta\alpha_f = 2\pi$ between 0 and $2\pi Z_R$ (for each incremental variation $\Delta\alpha_f$ the angle δ evolves between 0 and 2π) then a certain position of all Z_R 2D profiles of the rotary pins placed on the rotor are obtained, as Fig. 4 indicates by simulation. Figure 4 is a completion of Fig. 3. If the angle γ_f is changed then mainly the family of 2D rotary pins profiles (and their (H_{Cp}) hypocycloid as well) rotates around the origin of FCCS, as Fig. 5 proves (for $\gamma_f = 0$) by comparison with Fig. 4.

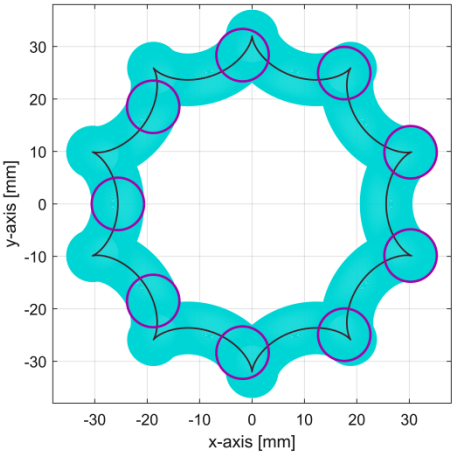

Fig. 4 – A completion of Fig. 3: the surface covered by *4500* equidistant 2D rotary pin profiles and a position of all Z_R 2D rotary pin profiles placed on the rotor.

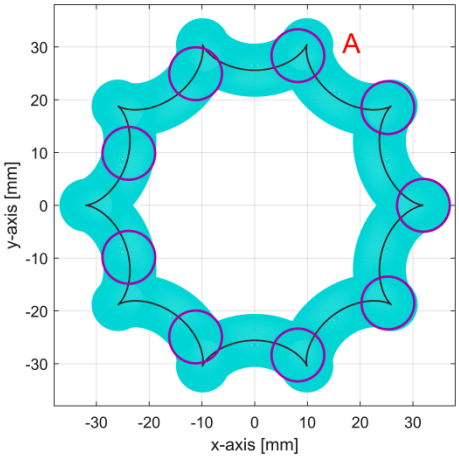

Fig. 5 – The simulation result from Fig. 4 using $\gamma_f = 0$.

A first obvious conclusion is available here: the external envelope of the family of these 2D rotary pin profiles (cyan colored area) is exactly the internal 2D profile of the ring gear (as cycloidal ring) having $Z_S = Z_R + 1$ teeth (10 teeth on Figs. 4 and 5). A second evident conclusion is available: the hypocycloid (H_{Cp}) describes exactly the trajectory of a cylindrical milling tool (having exactly the radius r_p) during an internal 2D contour milling for cycloidal ring manufacturing on CNC machines. This trajectory is analytically described with Eq. (10) and (11). For some reasons exposed here below, the hypocycloid (H_{Cp}) is replaced frequently with a distorted hypocycloid. However we should mention that in the manufacturing process defined above usually is indicated to use a milling tool with radius r_{mt} smaller than r_p in order to avoid the instability of cutting process. That is why rather in manufacturing is convenient to use the internal profile of the cycloidal ring. The 2D path (trajectory) of the tool axis (different by (H_{Cp}) if $r_{mt} < r_p$) is automatically calculated using a CAM software.

4. An approach on the description of the 2D profile of cycloidal ring

A simple method can be formulated in order to detect the description of 2D internal cycloidal ring profile as external envelope of the family of 2D rotary pin profiles. It uses a rotary semi straight line (RSSL) with the origin placed in the origin of FCCS, having an incremental variable angle θ related to the x-axis (initially $\theta=0$). According with Fig. 6 (based on a zoomed-in detail in area A from Fig. 5) this RSSL intersects some circles inside the family of 2D rotary pin profiles. Among all intersection points, only the one farthest from the origin is selected (P_{CRg} in Fig. 6). With certainty this point (having the coordinates $x_{CRgf}(\theta)$ and $y_{CRgf}(\theta)$ in FCCS) belongs to the 2D profile of the cycloidal ring.

Mainly three problems should be solved using analytic geometry: firstly the identification of circles from the family of 2D rotary pin profiles which intersect (RSSL) in two points should be done, secondly the coordinates of the intersection points should be calculated and thirdly the farthest point from the origin should be selected.

For each successive position of (RSSL) which rotates incrementally (with the increment $\Delta\theta$ which ensure the evolution of θ between 0 and 2π) the coordinates $x_{CRgf}(\theta)$ and $y_{CRgf}(\theta)$ of a point placed on 2D profile of cycloidal ring is obtained. This profile has a number of $2\pi/\Delta\theta$ points. The smaller the increments $\Delta\alpha_f$ and $\Delta\theta$ are, the higher description of 2D profile of the cycloidal ring is obtained. Figure 7 presents a completion of Fig. 6 with the 2D profile of the cycloidal disc (the red coloured curve) with a line segments between two successive points.

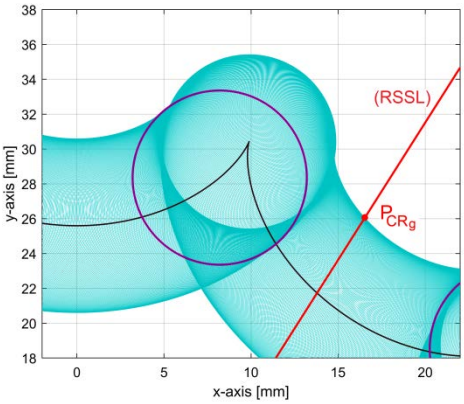

Fig. 6 – About the detection of a generic point P_{CRg} on 2D profile of the cycloidal ring. A completion of Fig. 5 in zoomed-in area A.

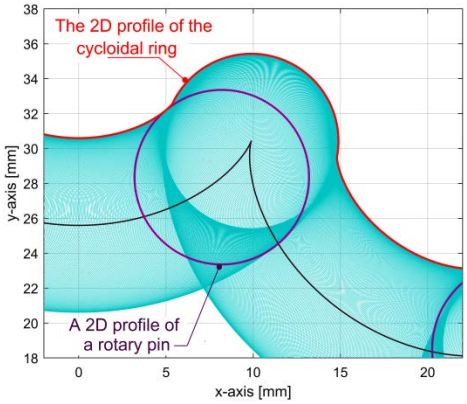

Fig. 7– A completion of Fig. 6 with the 2D profile of the cycloidal ring.

The entire 2D profile of the cycloidal ring from Fig. 7 is described with 5000 points ($\Delta\theta=2\pi/5000$ and $\Delta\alpha_f=2\pi/500$ for 4500 2D profile of rotary pins).

This entire 2D profile of the cycloidal ring is described on Fig. 8, a completion of Fig. 5, or a zoomed-out of Fig. 7. Figure 9 depicts only a position of 2D profiles of the rotary pins (already depicted in Figs. 4 and 5), the 2D profile of the cycloidal ring partially depicted in Fig. 7, the basic circle (S) and the rolling circle (R). We should mention that in Fig. 9 because $r_{pp}=r_R$ the circles (R) and (P) coincides.

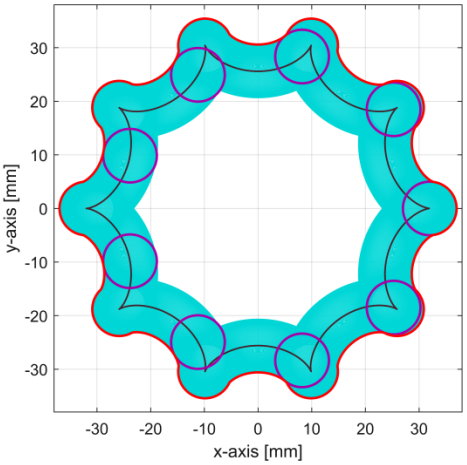

Fig. 8 – A completion of Fig. 5 with the entire 2D profile of the cycloidal ring.

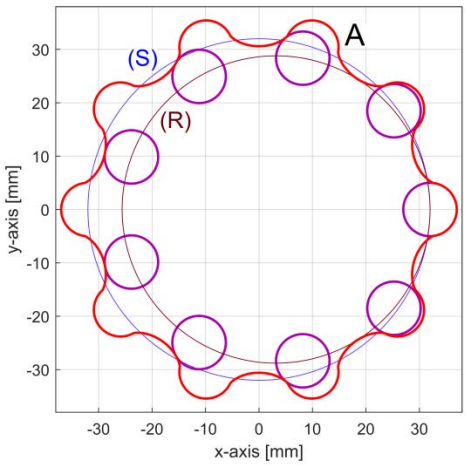

Fig. 9 – A selection from Fig. 8: 2D profile of cycloidal ring, a position of 2D profiles of the rotary pins placed on the rotor, the basic circle (S) and the rolling circle (R).

In Fig. 9 a gearing position between the rotor (with $Z_R=9$) and the stator ($Z_s=10$) of CR is depicted. Except one pin (having the center in the point P_t each other rotary pins touch the internal cycloidal ring profile in a single point. If the pins are fixed (they cannot rotate around their own axes) and if there is not backlash in gear (as it would be desirable) then there is a relative big slipping friction between these pins and the cycloidal ring. The using of rotary pins replaces the slipping friction with a (much smaller) rolling friction. Frequently in CR some bearings play the role of rotary pins.

A zoomed-in detail of Fig. 9 in area A (depicted in Fig. 10) shows two points of discontinuity P_{d1}, P_{d2} on each tooth of the 2D profile of cycloidal ring. The presence of these points does not damage the correct gearing but it is possible that the contact pressure developed here implies the danger of local pitting (or contact fatigue as well). In order to avoid this danger it is possible to eliminate these discontinuities by a so called positive profile shifting. The 2D profile of the cycloidal ring is generated using a diminished radius of rolling

circle (R) (as $r_R=r_{pp}-s$ with s being the profile shifting), and a diminished radius r_S of basic circle (S) but keeping the ratio $r_S/r_R=1-1/Z_R$, according with Eq. (4).

The effect of a positive profile shifting is depicted by simulation in Fig. 11 (a reconstruction of Fig. 10, with $s=6$ *mm*). As consequence of this positive shifting, the discontinuities on 2D profile of the cycloidal ring disappear. Because of shifting, now the circles (P) and (R) no longer coincide.

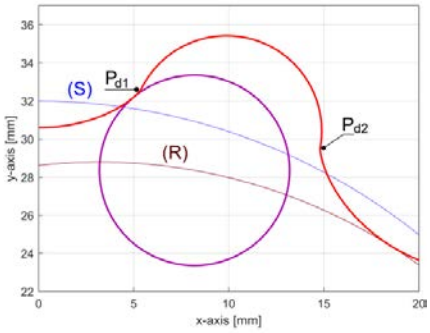

Fig. 10 – A in zoomed-in detail in the area A of Fig. 9.

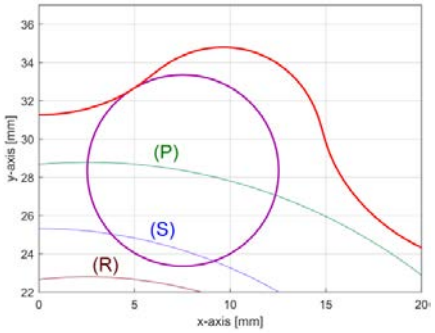

Fig. 11 – A reconstruction of Fig. 10, with a positive shifting ($s=6mm$) of 2D profile of the cycloidal ring.

Figure 12 presents the entire 2D profile of the cycloidal ring (a reconstruction of Fig. 9 with $s=6$ *mm* or a zoomed-out detail of Fig. 11. For a better description of the effects of positive shifting, Fig. 13 presents an overlapping of 2D profiles (pins on the rotor and stator) from Figs. 9 (in red) and 12 (in blue).

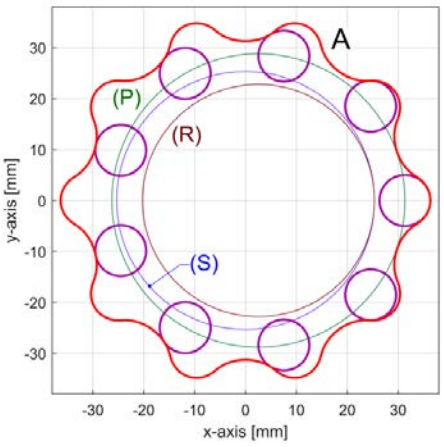

Fig. 12 – A reconstruction of Fig. 9, with a positive shifting of 2D profile of the cycloidal ring ($s=6mm$).

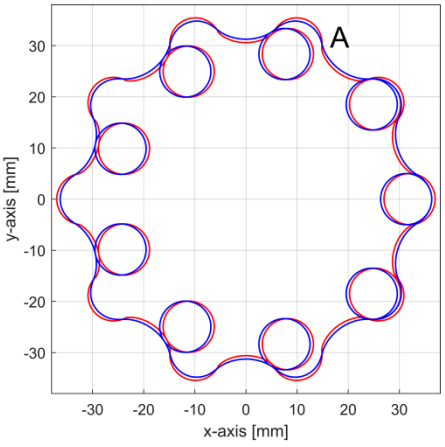

Fig. 13 – An overlapping of 2D profiles (pins on the rotor and stator) from Fig. 9 (in red) and Fig. 12 (in blue).

The only changes between Figs. 9 and 12 is the profile shifting. This shifting implies also the decreasing of teeth height on cycloidal ring. This decreasing is more evident in Fig. 14, as a zoomed-in detail of Fig. 13 in area A. The trajectory of a rotary pin from the stator involved in the definition of cycloidal ring 2D profile from Fig. 9 (a hypocycloid (H_{Cp})) becomes now a distorted hypocycloid (dH_{Cp}) due to the shifting. For a rotor position related to the stator all the rotary pins are placed in different places on the same distorted hypocycloid (dH_{Cp}).

The setting of the shifting value *s* is a matter of CR optimisation, a possible topic for a future research.

Because the rotor is placed out-of-center related by fixed rotation joint (O_1) of the carrier, there is a relatively strong mechanical unbalance inside the CR (or dynamic imbalance, produced when the carrier rotates with high rotation speed) which mandatory should be eliminated. Usually two identically rotors are used, with 180 degrees out of phase on their identical carriers (related by their relative angular position), with the same number of rotary pins, the same value of r_p and r_{pp}, being in gear with the same cycloidal ring. Figure 15 depicts the 2D profile of the cycloidal ring from Fig. 12 and the 2D profiles of the rotary pins for each of two rotors (in blue and cyan).

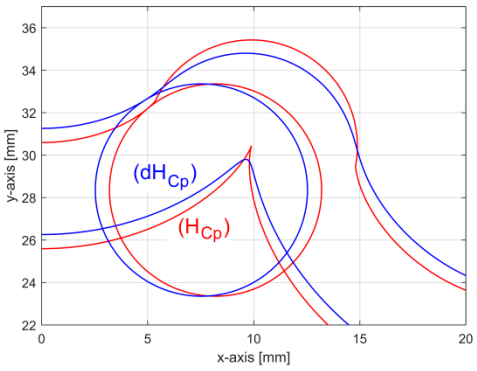

Fig. 14 – A zoomed-in detail on Fig. 13 (in area A).

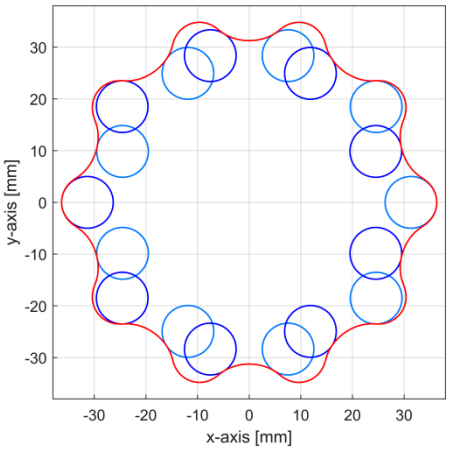

Fig. 15 – A conceptual description of a CR with two rotors. On each rotor Z_R rotary pins are placed.

It is easy to observe that the 2D profiles of the pins from a rotor are found by 2D mirroring from the positions of the other rotor. In the particularly position from Fig. 15 the mirror line is *y*-axis of FCCS. Apart from the fact that it helps to eliminate the dynamic imbalance, the second rotor increases also the maximum output torque which a CR is able to deliver.

A similar study on different design conditions for a CR (different r_p, Z_R and s values) can be done by this type of simulation.

5. An approach on the design of a 3D CAD model for a cycloidal ring based on its 2D profile in transverse section

The 2D profile previously defined in Fig. 12 can be used directly in cycloidal ring manufacturing (by contour milling on CNC machines) or indirectly in the generation of the 3D CAD model of the cycloidal ring, for different purposes (computer aided manufacturing, CR simulation and optimisation, etc.). When we talk about contour milling, this 2D profile helps to define the milling tool pathway. As specified previously, now the distorted hypocycloid (dH_{Cp}) can be in theory the milling tool pathway if this tool has exactly the radius r_p. In order to avoid dynamic instability of the milling process, the radius of milling tool should be mandatory smaller than r_p.

A simple approach in CAD allows the conversion of the 2D profile from Matlab in internal shape of the cycloidal ring. This 2D profile is exported in an appropriate format to the CAD software. With the 3D extrusion command this profile is converted in the inner surface of a 3D model for the cycloidal ring. Figure 16 presents a conceptual view of the cycloidal ring having as inner transverse section the 2D profile already defined before in Fig. 12. Figure 17 presents a view on a conceptually CR in a 3D CAD model with a single rotor (in blue, having $Z_R=9$ rotary pins in red) being in gear with the cycloidal ring from Fig. 16 (in cyan).

Fig. 16 – A conceptual view on 3D CAD model of a cycloidal gear having the transverse section the 2D profile from Fig. 12.

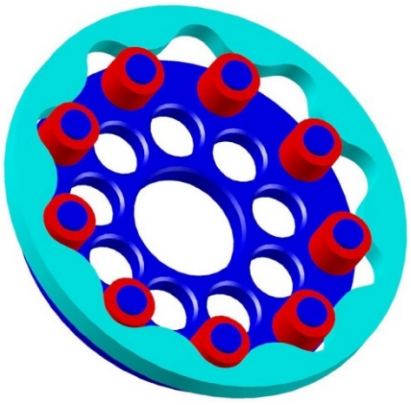

Fig. 17– A conceptual view on CR in a 3D CAD model with the rotor (in blue, having $Z_R=9$ red rotary pins) in gear with the cycloidal ring from Fig. 12.

The central hole is used to supply CR with input motion (having the rotary speed n_{in}), here being placed the rotary joint O_2 at the free end of the

carrier (Fig. 1). The other holes are used for the takeover of output motion (having the speed n_{out}). The rotary pins can be replaced by bearings.

6. Conclusions and future work

This paper continues some theoretical approaches on cycloidal reducers (CR) already presented in (Horodincă *et al.*, 2022). These approaches were focused on the finding out of the inner 2D profile of the cycloidal disc inside a CR where the stator (the ring gear being in gearing with the rotor) has rotary cylindrical pins as gear teeth.

A new approach on CR design is proposed in this paper based on a known working principle: the internal gearing between a rotor (as planet gear which is rotate by a carrier having Z_R cylindrical rotary pins as teeth) and a stator (fixed cycloidal ring) having an appropriate shape with $Z_S = Z_R + 1$ lobes as teeth. The main challenge solved in this paper is the finding out the geometrical description of the inner 2D profile of the cycloidal ring having positive shifting. In order to find out this profile first the family of rotary pins 2D transverse sections (circles) for a completely rotation of the carrier (where the rotor is placed) is generated by computer aided simulation. The centers of these circles are placed on a closed distorted hypocycloid. Secondly, the description of the external envelope of this family of all rotary pins positions is found, as being the description of the 2D profile of the cycloidal ring, given through the coordinates of its points in a fixed Cartesian coordinates system. This 2D profile is useful either for manufacturing of the internal shape of the cycloidal ring by contour milling on CNC machines either for the synthesis of the 3D CAD model of the cycloidal ring or CR as well.

A future work intends to valorise these achievements in CR design and manufacturing for a specific experimental purpose: the increasing of power efficiency. Particularly the value of profile shifting *s* will be optimised.

REFERENCES

Allotta B., Fiorineschi L., Papini S., Pugi L., Rotini F., Rindi A., *Redesigning the Cycloidal Drive for Innovative Applications in Machines for Smart Construction Yards*, World Journal of Engineering, **18**, *2*, 302-315 (2021).

Horodincă M., *An Approach on Simulation of Sine Gear Profile Used on Cylindrical Gears*, Buletinul Institutului Politehnic din Iași, **66 (70)**, *2*, s. Machines Manufacturing, 37-52 (2020).

Horodincă M., Bumbu N.E., Munteanu A., Chitariu D.F., Chifan F., *A Study on the Synthesis of 2d Profiles for Cycloidal Discs Used in Cycloidal Reducers*, Buletinul Institutului Politehnic din Iași, **68 (72)**, *4*, s. Machines Manufacturing, In press corrected proof (2022).

Huang C.H., Tsai S.J., *A Study on Loaded Tooth Contact Analysis of a Cycloid Planetary Gear Reducer Considering Friction and Bearing Roller Stiffness*, Journal of Advanced Mechanical Design, Systems, and Manufacturing (Bulletin of the JSME), **11**, *6*, 17-00213 (2017).

Litvin F.L., Feng P.H, *Computerized Design and Generation of Cycloidal Gearings*, Mechanism and Machine Theory, **31**, *7*, 891-911 (1996).

Mackic T., Blagojevic M., Babic Z., Kostic N., *Influence of Design Parameters on Cyclo Drive Efficiency*, Journal of the Balkan Tribological Association, **19**, *4*, 497-507 (2013).

Petrovic N., Blagojevic M, Marjanovic N., Matejic M., *Parametric Drawing of a Cyclo Drive Shortened Equidistant Epitrochoid Gear*, Proc. of the 7th International Quality Conference, May 24th, 2013 Center for Quality, Faculty of Engineering, University of Kragujevac, Serbia, 303-308.

Shin J.H., Kwon S.M., *On the Lobe Profile Design in a Cycloid Reducer Using Instant Velocity Center*, Mechanism and Machine Theory, **41**, *5*, 596-616 (2006).

Wang H., Zhao-Yao S., Bo Y., Hang X., *Transmission Performance Analysis of RV Reducers Influenced by Profile Modification and Load*, Applied Sciences, **9**, *19*, 4099 (2019).

UN STUDIU ASUPRA PROFILULUI 2D ÎN SECȚIUNE TRANSVERSALĂ PENTRU STATORUL UNUI REDUCTOR CICLOIDAL

(Rezumat)

Lucrarea extinde elementele de studiu teoretic al reductoarelor cicloidale deja introduse anterior (Horodincă *et. al.*, 2022), cu privire la sinteza profilelor 2D ale secțiunii transversale ale suprafeței interioare de contact (folosită în angrenare) de pe stator (roata inel fixă). Acest profil este conjugat prin angrenarea profilului de rotor al cărui (Z_R) dinți sunt materializați cu elemente cilindrice rotative (în particular rulmenți). Utilizarea acestui tip de dantură pe rotor are drept scop substituirea frecării de alunecare în angrenaj cu cea de rostogolire, cu consecințe favorabile asupra eficienței energetice a reductorului (creșterea randamentului) și asupra durabilității acestuia. Profilul 2D al secțiunii transversale a statorului rezultă definit punct cu punct ca înfășurată la exterior a tuturor pozițiilor secțiunilor transversale (cercuri) ale dinților rotorului cu profil deplasat, ca o curbă cicloidală închisă cu Z_S lobi (hipocicloidă deformată). Acest profil este util fie pentru fabricarea efectivă a statorului reductorului (prin frezare interioară 2D după contur pe mașini cu comandă numerică) fie pentru realizarea modelului 3D CAD a reductorului în vederea realizării elementelor de simulare și analiză a funcționării în diferite condiții structurale.